Bioorganic & Medicinal Chemistry Letters 24 (2014) 2525–2529

Contents lists available at ScienceDirect

Bioorganic & Medicinal Chemistry Letters

journal homepage: www.elsevier.com/locate/bmcl

Identification of a new series of potent diphenol HSP90 inhibitors by fragment merging and structure-based optimization

Jing Ren [a,†], Jian Li [b,d,†], Yueqin Wang [c,†], Wuyan Chen [d], Aijun Shen [c], Hongchun Liu [c], Danqi Chen [a], Danyan Cao [a], Yanlian Li [a], Naixia Zhang [a], Yechun Xu [d], Meiyu Geng [c,*], Jianhua He [b,*], Bing Xiong [a,*], Jingkang Shen [a,*]

[a] Department of Medicinal Chemistry, National Key Laboratory of New Drug, Shanghai Institute of Materia Medica, Chinese Academy of Sciences, 555 Zuchongzhi Road, Shanghai 201203, China
[b] Shanghai Institute of Applied Physics, Chinese Academy of Sciences, 239 Zhangheng Road, Shanghai 201204, China
[c] Division of Antitumor Pharmacology, Shanghai Institute of Materia Medica, Chinese Academy of Sciences, 555 Zuchongzhi Road, Shanghai 201203, China
[d] CAS Key Laboratory of Receptor Research, Drug Discovery and Design Center, Shanghai Institute of Materia Medica, Chinese Academy of Sciences, 555 Zuchongzhi Road, Shanghai 201203, China

ARTICLE INFO

Article history:
Received 8 January 2014
Revised 26 February 2014
Accepted 31 March 2014
Available online 8 April 2014

Keywords:
Heat shock protein
HSP90
Fragment-based drug discovery
Anticancer

ABSTRACT

Heat shock protein 90 (HSP90) is a molecular chaperone to fold and maintain the proper conformation of many signaling proteins, especially some oncogenic proteins and mutated unstable proteins. Inhibition of HSP90 was recognized as an effective approach to simultaneously suppress several aberrant signaling pathways, and therefore it was considered as a novel target for cancer therapy. Here, by integrating several techniques including the fragment-based drug discovery method, fragment merging, computer aided inhibitor optimization, and structure-based drug design, we were able to identify a series of HSP90 inhibitors. Among them, inhibitors **13**, **32**, **36** and **40** can inhibit HSP90 with IC_{50} about 20–40 nM, which is at least 200-fold more potent than initial fragments in the protein binding assay. These new HSP90 inhibitors not only explore interactions with an under-studied subpocket, also offer new chemotypes for the development of novel HSP90 inhibitors as anticancer drugs.

Heat shock protein 90 (HSP90) belongs to a large family of heat shock proteins with molecular weight around 90 kDa, and functions as a molecular chaperone to fold and maintain proper conformations of many 'client' proteins.[1–3] HSP90 is upregulated by heat and other stressors to protect cells against these damaging effects, and it consists of two isoforms: HSP90α is an inducible form overexpressed in many cancer cells, while HSP90β is the constitutive form.[4,5] As one of the most abundant member of heat shock proteins, HSP90 has been extensively studied and reported to have at least 280 client proteins.[6] Among them, 48 are involved in cell growth and various signaling cascades. Some of its clients are notorious oncogenes, including several validated cancer drug targets such as HER-2, Bcr-Abl, VEGFR, EGFR. Besides, the more sensitive clients are usually those mutated unstable proteins involved in aberrant signaling transduction in tumor cells. Since inhibition of HSP90 can lead to the degradation of a large collection of oncogenic proteins, it has been considered as a promising target for cancer therapy.[7,8] The most attractive strength of HSP90 inhibitors is that they can not only simultaneously affect several aberrant signaling pathways essential for cancer development, may also reduce the possibility of acquiring resistance in tumor cells induced by some targeting drugs treatment.[9]

Currently, many HSP90 inhibitors have been discovered and more than 10 drugs are now in clinical trials. Figure 1 lists several diversified HSP90 inhibitors,[10,11] and they are all bound to the ATP site of the HSP90 N-terminal ATPase domain to impede the chaperone function of HSP90. As the prototype of several synthetic inhibitors, radicicol (**2**) contains a core fragment, dihydroxyphenyl group which forms extensive hydrogen bonding interactions with the ATP binding site of N-terminus of HSP90. Beside of these inhibitors inspired by natural products, fragment-based drug discovery (FBDD) is also a popular strategy in the HSP90 inhibitor development, which was adopted to discover AT13387(**4**) in Astex pharmaceutical[12] and SNX-5422(**5**) in Serenex.[13] Here we report an application of FBDD approach to identify new series of dihydroxyphenyl-based HSP90 inhibitors, which initially designed by merging two bioactive fragments identified

* Corresponding authors. Tel./fax: +86 21 50806600 5412 (B. X).
E-mail addresses: mygeng@simm.ac.cn (M. Geng), hejh@sinap.ac.cn (J. He), bxiong@simm.ac.cn (B. Xiong).
† These authors contributed equally to this work.

http://dx.doi.org/10.1016/j.bmcl.2014.03.100
0960-894X/

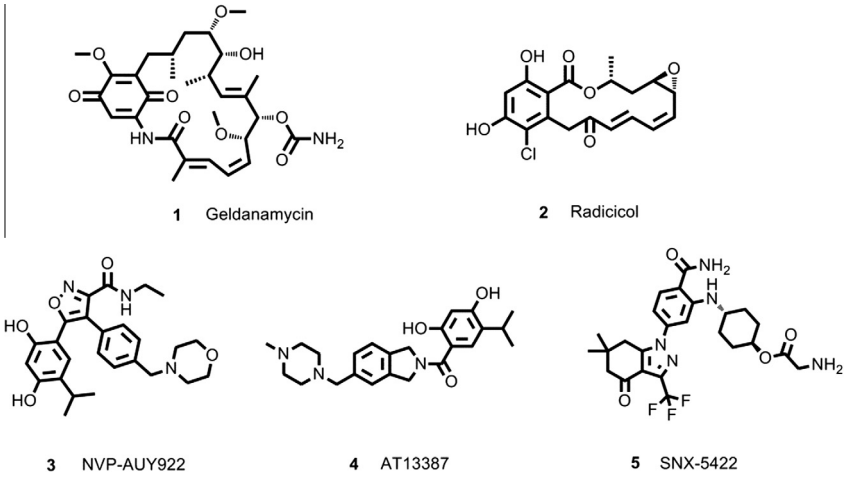

Figure 1. HSP90 inhibitors.

from crystallography-based fragment screening, and followed with the optimization guided by structure-based drug design methods.

To apply the FBDD approach, we firstly analyzed crystal structures of complexes of HSP90 and its inhibitors deposited in PDB database. Through this, it was found that all inhibitors have an essential chemical moiety forming two hydrogen bonds with the residue ASP93 of HSP90. Based on this critical interaction pattern, we screened the ChemDiv commercial available database with this pharmacophore, and scrutinized its novelty and synthesis accessibility of fragment hits. After that, we purchased and synthesized about twenty promising fragments as our small HSP90 focused library. By utilizing the co-crystallization and screening with X-ray crystallography method,[14] we were able to identify several fragments bound in the ATP site of HSP90 in solved crystal structures, and two of them were illustrated in Figure 2. To our surprise, fragment **6** binds to HSP90 in an unexpected way. Before obtained the co-crystal structure of **6** with HSP90, we speculated that it would bind to the position similar to the isoxazole ring of AUY922; while as illustrated in Figure 2A, in the complex crystal structure it rotates around the phenol ring and enables the [12,4]triazolo[4,3-*a*]pyridine group situating at a small subpocket that usually accommodates the isopropyl group in compounds AUY922 and AT-13387. Besides, it was found the triazolopyridine ring forms a π–π stacking interaction with residue PHE-138 and one of the nitrogen atoms in triazole ring form two hydrogen bonds with residue ASN-51 through a structural water molecule. By overlapping two complex structures of fragments **6** and **7** (Fig. 2D), we can identify the phenol rings match very well. Consequently, we designed compounds **8** and **9** by merging these two fragments, and expected it to have improved binding affinity to HSP90. As listed in Table 1, from the fluorescence polarization (FP) assay, compound **8** and its analog **9** surprisingly showed lower activities against HSP90 than the fragments.

To gain an understanding why the binding affinity is considerably low, we crystallized and successfully solved the co-structure of HSP90 with compound **9** (Fig. 2E). As shown, the compound **9** binds to the N-terminal of HSP90 as expected, with the triazolopyridine ring situated at the same position of fragment **6**. Based on this crystal structure, we use the computational chemistry

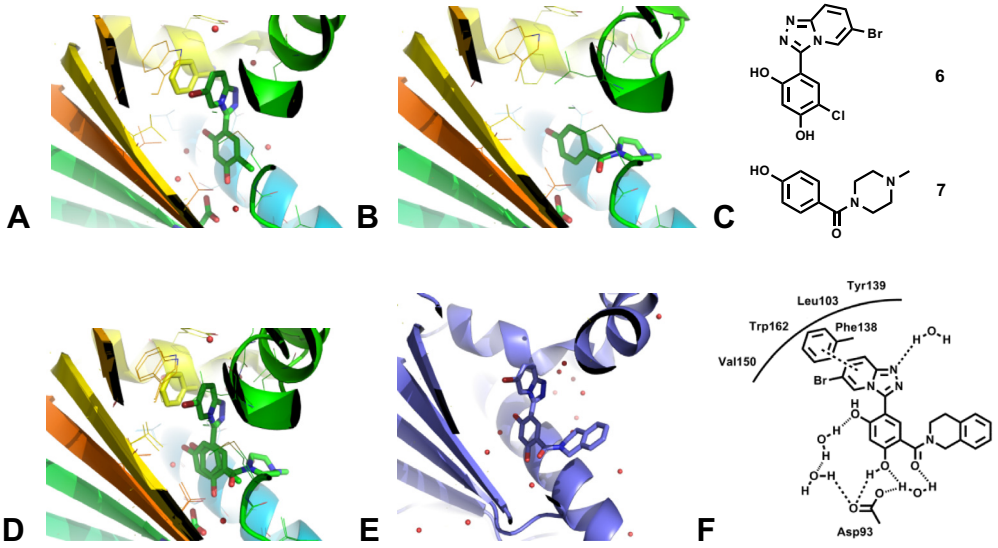

Figure 2. Co-crystal structures of HSP90 with compounds **6**, **7** and **9**. The HSP90 was shown in cartoon style and the ligands **6**, **7** and **9** were shown in stick. (A) The co-crystal structure of HSP90 with **6** (PDB ID: 4L91). (B) The co-crystal structure of HS90 with **7** (PDB ID: 4L94). (C) The chemical structures of fragments **6** and **7**. (D) Superimposition of co-crystal structures of **6** and **7**. (E) Co-crystal structure of HSP90 with **9** (PDB ID: 4L8Z). (F) The 2D diagram of interactions between HSP90 and compound **9**.

Table 1
The fluorescence polarization assay of the identified active fragments and compounds from initial optimization

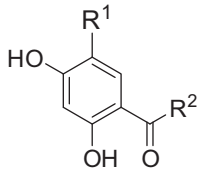

6-15

Compd	R^1	R^2	FP IC_{50}[a] (μM)
8	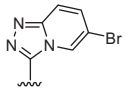	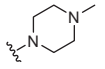	8.8 ± 2.1%@5 μM[b]
9	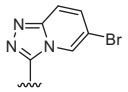	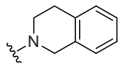	18.7 ± 5.1%@5 μM[b]
10		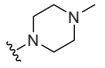	0.63 ± 0.08
11		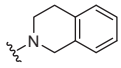	0.13 ± 0.01
12		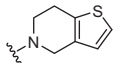	0.33 ± 0.02
13		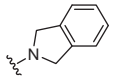	0.038 ± 0.006
14		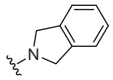	0.13 ± 0.01
15		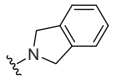	0.25 ± 0.03

[a] All the inhibition ratios or IC_{50} values were obtained from triple measurements. The compounds Geldanamycin and NVP-AUY922 were used as control, with IC_{50} values 74.0 ± 7 nM and 8.0 ± 0.2 nM, respectively.
[b] The inhibition ratio measured with FP assay method at ligand concentration 5 μM.

methods to quantify two important components of the protein–ligand binding free energy, namely the binding interaction energy and solvation free energy, of ligand **9** with or without the triazolopyridine group. The Glide docking program[15] in Schrödinger software package was used to calculate the protein–ligand binding energy. Since we solved the crystal structure of ligand **9** bound to the N-terminal of HSP90, the SCORE-ONLY mode was used to obtain the binding interaction energy. From the calculation, it was found that the non-covalent interaction energy between compound **9** and the N-terminal of HSP90 is −68.78 kcal/mol, and the large contribution stems from van der Waals interactions (−56.83 kcal/mol). While for the virtual compound by deleting the triazolopyridine group (see chemical structure 9v in Supporting materials) from ligand **9**, its interaction energy is −48.77 kcal/mol. The large difference of non-covalent interactions between two compounds is rooted from the difference of their van der Waals interactions (ligand **9** is −20.25 kcal/mol lower), while the coulomb electrostatic interactions are almost the same (ligand **9**: −11.95 kcal/mol; the virtual compound without the triazolopyridine group: −12.18 kcal/mol). From these docking energy calculations, it was shown that the binding of triazolopyridine at the ATP site of HSP90 is enthalpy favorable and the electrostatic interaction between triazolopyridine group and HSP90 is less important than the van der Waals interactions. As pointed by numerous analyses that the enthalpy and entropy compensation is a common phenomenon in protein–ligand interactions[16] that says favorable enthalpy interactions such as hydrogen bonding, π–π stacking can countpoise by the reduction in entropy contribution due to restriction of the flexibility of the receptor. Therefore, the actually improvement in binding free energy of compound **9** may be low than the enthalpy contribution since the triazolopyridine group clearly hinders the mobility of its surrounding residues of HSP90. Nevertheless, we thought the binding interaction of triazolopyridine group is not the destructive factor accounting for the low activity of compound **9**.

Then we performed the solvation free energy calculations on compound **9**. By utilizing the density functional M06-2X at 6-31+G(d) level combined with the SMD solvation model[17] implemented in Gaussian program, we found that compound **9** has a low solvation free energy about −26.66 kcal/mol, which indicated that when binding to the HSP90, the compound needs to overcome a large desolvation effect to transfer from aqueous solution to the protein binding site. The solvation free energy of the virtual compound without the triazolopyridine group is −19.72 kcal/mol. Taking together, it means that adding the triazolopyridine group needs to supply about 7 kcal/mol desolvation free energy. Therefore, in the next round of optimization, we focused on the issue of the hydrophilicity of the compounds, and tried to reduce the ligand solvation free energy to improve the binding affinity to HSP90.

Based on the previous SAR of HSP90 inhibitors,[18] the tetrahydroisoquinoline in compound **9** is not the optimal for binding. Therefore, together with above mentioned rationale, several hetero-aromatic rings were used to substitute the [12,4]triazolo[4,3-*a*]pyridine group, and produced compounds **10**–**15**. Comparison of compounds **10** to **8** or **11** to **9**, the only difference occurs at the triazolopyridine ring substituted with the indole group; the binding activities from FP assay are dramatically improved. This is consistent with the calculation that the solvation free energy of compound **11** is −13.98 kcal/mol, much less than the value of compound **9** (−26.66 kcal/mol). Similar trend can be deduced from the inhibition activities of **13**–**15**. Compounds **14** and **15** are about 3 and 7-fold less active than ligand **13** respectively, which reinforces the hydrophobic property of the fused bicyclic ring is critical for the binding. From compounds **10**–**13** in Table 1, it was found that compound **13** with isoindoline group at R^2 is the most potent inhibitor, consistent with the data reported in the previous structure–activity relationship about R^2 group.[12] Consequently, we selected compound **13** to carry out the further optimization by attaching various functional groups to the indole moiety.

The synthesis route of compounds in Table 2 is outlined in Scheme 1 (see the Supporting material for details). Generally, the synthesized compound **16** was hydrolyzed with lithium hydroxide to give compound **17**. Compound **18** was prepared by coupling the key intermediate **17** with isoindoline using standard EDC/HOBt coupling conditions. After coupling of **18** with different substituted indoles,[19] followed by de-protection of the benzyl protecting groups, the final product **28**–**36** were obtained.

Inspecting the co-crystal structure, it was thought that the subpocket accommodating the indole ring cannot permit a large substituent on the indole, especially at 6-, 7-position of indole ring. Based on the in silico modeling, we prepared 9 compounds with various substituents at three positions of indole. As listed in Table 2, modification of the R^1-position of indole with linear polar groups (compounds **28**–**30**) decreases the binding affinity considerably, at least 30-fold less active than the parent compound **13**, especially the compound with acidic group (**30**). Due to the limited

Table 2
The fluorescence polarization binding assay of compounds **28**–**36l**

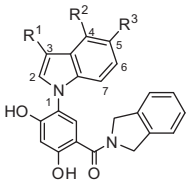

Compd	R^1	R^2	R^3	FP IC_{50}[a] (μM)
28		H	OMe	1.5 ± 0.33
29	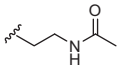	H	OMe	56.9% ± 6.3%@1 μM[b]
30		H	H	14.1% ± 7.7%@1 μM[b]
31	H	Br	H	0.07 ± 0.01
32	H	NO_2	H	0.039 ± 0.0005
33	H		H	0.13 ± 0.01
34	H		H	0.62 ± 0.09
35	H	H	Br	0.078 ± 0.005
36	H	H	Me	0.038 ± 0.003

[a] All the inhibition ratios or IC_{50} values were obtained from triple measurements.
[b] The inhibition ratio measured with FP assay method at ligand concentration 1 μM.

volume of the subpocket accommodating the indole ring, as indicated in Table 2, the inhibitory activity is very sensitive to the substitution at R^2- or R^3-position of indole. The bromine atom at these positions of the indole ring is tolerable, both with IC_{50} value about 70 nM (**31** and **35**). The 4-nitro indole can maintain the equipotency against HSP90 in FP assay, but the activities of compounds **33** and **34** with a slightly large group at R^2-position of indole is lower than compound **13**, decrease about 4- and 20-fold, respectively. **36** with methyl group at R^3-position of indole is also tolerable with similar IC_{50} value (38 nM).

From the co-crystal structure of HSP90 bound with compound **9**, the π–π stacking involving the residue PHE138 is important for van der Waals interactions. Due to the ligand stacking part is largely at the six-membered ring of indole, therefore, the ring-opening approach was taken to further modify the indole ring by changed it to phenyl-amino group. With this effort, compounds **40**–**42** were prepared via palladium catalyzed Buchwald–Hartwig amination[20,21] from the intermediate **18**, and followed by deprotection.

As shown in Table 3, the compound (**40**) bearing aniline moiety is the most potent inhibitor against HSP90 in current study, with the IC_{50} about 21 nM in the FP assay. Compound **41** with methyl group substituted at R^1 position shows moderate inhibition (IC_{50} = 71 nM), while the compound (**42**) with di-chlorine substituted phenylamino group decreases the potency about 6-fold (IC_{50} = 190 nM). Although we only synthesized few compounds, to the best of our knowledge, this modification is interesting as it provided new ideas for HSP90 inhibitor development, which may also enable other researchers to design substituted phenylamino groups or novel heterocycles at this position.

We investigated the druglikeness of these series by selecting 8 potent compounds to check their metabolic stability properties—the clearance ratio in human and mouse liver microsomes as well as the inhibitions against five cytochrome P450 isoenzymes. In Table 4, all tested molecules demonstrated low clearance ratio in human or rat liver microsomes. Although all compounds showed no more than 50% inhibition at concentration 10 μM against the abundant CYP isoenzymes 3A4 and 2D6, they did process unfavorable inhibitions towards other three isoenzymes 2C9, 1A2, and 2C19. We also checked the time-dependent inhibition (TDI) of these compounds, and found that only compound **32** has TDI inhibition to 2C19. Taking together, we selected compounds **13**, **31**, **36** and **42** for further cellular activity test, as these compounds demonstrate slightly better stability profiles than others.

From Table 5, it was found that the selected four compounds have similar inhibitory activities, with GI_{50} around 10 μM against four cancer cell lines. By comparing to the potent cellular proliferation activities of the HSP90 inhibitors in clinical trials,[11] we speculate these compounds may have poor cell permeability issues as there is a large gap between cellular activity and protein binding activity. Further membrane permeability assay will verify this hypothesis, and may shed the light on the direction of optimization.

In summary, by employing the fragment-based drug discovery approach, we were able to identify two binding fragments. Scrutinizing the co-crystal structures of these two fragments with N-terminal ATPase domain of HSP90, it was found that two fragments situated at different subpocket in ATP binding site, and their common pharmacophore-phenol ring fitted very well. Apparently merging two fragments to form compound **9** were proved not to

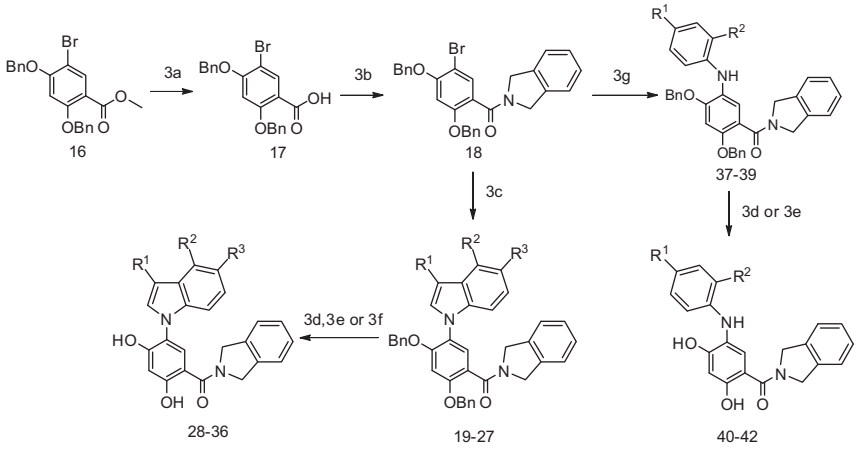

Scheme 1. Synthesis of compounds **28**–**36** and **40**–**42**. Reagents and conditions: (**3a**) LiOH, MeOH,H_2O, reflux, 99%; (**3b**) isoindoline, EDCI, HOBt, DIPEA, DCM, rt, 70%; (**3c**) indoles, K_3PO_4, CuI, (+/−)-trans-1,2-Diaminocyclohexane or (1*R*,2*R*)-*N*,*N*′-Dimethyl-1,2-cyclohexane-diamine, toluene, reflux, 40–85%; (**3d**) H_2, Pd/C, MeOH, rt, 35–85%; (**3e**) BCl_3, DCM, 0 °C, 19–42%; (**3f**) BBr_3, DCM, −78 °C, 13%; (**3g**) aniline, Pd2(dba)$_3$, *t*-Bu_3P or X-phos, NaOBu-t, dioxane, 120 °C, 36–75%.

Table 3
The fluorescence polarization binding assay of compounds **40–42**

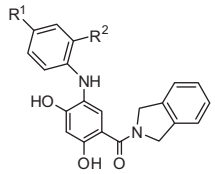

Compd	R^1	R^2	FP IC_{50}[a] (μM)
40	H	H	0.021 ± 0.005
41	Me	H	0.071 ± 0.003
42	Cl	Cl	0.19 ± 0.04

[a] All the inhibition ratios or IC_{50} values were obtained from triple measurements.

Table 4
The in vitro metabolic stability study of the selected compounds

Compd (10 μM)	HLM[a] Stability Clint(ul/min/mg protein)	RLM[b] Stability Clint(ul/min/mg protein)	Direct inhibition mean (inhibition ratio)					Time-dependent inhibition
			3A4	2D6	2C9	1A2	2C19	
13	13	25	37%/17%	14%	73%	52%	60%	No inhibition
31	0	49	33%/22%	19%	54%	34%	70%	No inhibition
32	22	6	35%/8%	50%	74%	47%	89%	2C19
35	18	16	15%/13%	32%	78%	48%	71%	No inhibition
36	0	42	26%/4%	7%	68%	28%	63%	No inhibition
40	2	12	19%/29%	22%	68%	72%	52%	No inhibition
41	0	0	40%/38%	7%	75%	61%	58%	No inhibition
42	0	16	39%/33%	5%	73%	40%	23%	No inhibition

[a] HLM is human liver microsome.
[b] RLM is rat liver microsome.

Table 5
The cellular antiproliferative activity of compounds **13**, **31**, **36** and **42**[a]

Compd	GI_{50} (μM)			
	HCT116	NCI-H3122	A549	BT-474
13	10.08 ± 0.17	7.53 ± 0.82	14.31 ± 1.57	7.25 ± 0.37
31	12.26 ± 2.15	9.67 ± 0.01	21.01 ± 2.02	8.52 ± 0.52
36	8.6 ± 1.69	7.53 ± 1.19	11.1 ± 1.69	7.07 ± 3.48
42	10.63 ± 0.3	10.12 ± 0.03	24.17 ± 1.69	6.31 ± 1.22

[a] Values represent mean ± standard deviation are calculated from experiments performed in triplicate.

be successful as the compound **9** is surprisingly less active than its parent fragment. To gain the knowledge about the reason of this phenomenon, computational modeling was adopted to calculate two important components in binding free energy: the binding interaction energy and ligand solvation free energy. Through the calculations, it was found that the destructive factor may be rooted from ligand solvation free energy. Therefore, in the next rounds of optimization, we focused on reducing the hydrophilic tendency of ligands, and successfully obtained several compounds were at least 200-fold more active than the initial fragments. These new series of HSP90 inhibitors are interesting as the ligands extend to a less explored subpocket, which may provide several potential chemotypes for HSP90 inhibitor development.

Acknowledgments

The authors wish to thank Dr. Haiyan Liu for her help in performing the in vitro PK study. We are grateful for financial support from 'Interdisciplinary Cooperation Team' Program for Science and Technology Innovation of the Chinese Academy of Sciences; the '100 Talents Project' of CAS to Y.X. The National Natural Science Foundation of China (Grant Nos. 81072580, 81273368 and 21272246); the National Science & Technology Major Project 'Key New Drug Creation and Manufacturing Program' of China (Grant No. 2014ZX09507-002).

Supplementary data

Supplementary data associated with this article can be found, in the online version, at http://dx.doi.org/10.1016/j.bmcl.2014.03.100.

References and notes

1. Feder, M. E.; Hofmann, G. E. *Annu. Rev. Physiol.* **1999**, *61*, 243.
2. Picard, D. *Cell. Mol. Life Sci.* **2002**, *59*, 1640.
3. Garrido, C.; Gurbuxani, S.; Ravagnan, L.; Kroemer, G. *Biochem. Biophys. Res. Commun.* **2001**, *286*, 433.
4. Pearl, L. H.; Prodromou, C. *Annu. Rev. Biochem.* **2006**, *75*, 271.
5. Moulick, K.; Ahn, J. H.; Zong, H.; Rodina, A.; Cerchietti, L.; Gomes DaGama, E. M.; Caldas-Lopes, E.; Beebe, K.; Perna, F.; Hatzi, K.; Vu, L. P.; Zhao, X.; Zatorska, D.; Taldone, T.; Smith-Jones, P.; Alpaugh, M.; Gross, S. S.; Pillarsetty, N.; Ku, T.; Lewis, J. S.; Larson, S. M.; Levine, R.; Erdjument-Bromage, H.; Guzman, M. L.; Nimer, S. D.; Melnick, A.; Neckers, L.; Chiosis, G. *Nat. Chem. Biol.* **2011**, *7*, 818.
6. da Silva, V. C.; Ramos, C. H. *J. Proteomics* **2012**, *75*, 2790.
7. Travers, J.; Sharp, S.; Workman, P. *Drug Discov. Today* **2012**, *17*, 242.
8. Hwang, M.; Moretti, L.; Lu, B. *Curr. Med. Chem.* **2009**, *16*, 3081.
9. Xu, W.; Neckers, L. *Clin. Cancer Res.* **2007**, *13*, 1625.
10. Hong, D. S.; Banerji, U.; Tavana, B.; George, G. C.; Aaron, J.; Kurzrock, R. *Cancer Treat. Rev.* **2013**, *39*, 375.
11. Biamonte, M. A.; Van de Water, R.; Arndt, J. W.; Scannevin, R. H.; Perret, D.; Lee, W. C. *J. Med. Chem.* **2010**, *53*, 3.
12. Woodhead, A. J.; Angove, H.; Carr, M. G.; Chessari, G.; Congreve, M.; Coyle, J. E.; Cosme, J.; Graham, B.; Day, P. J.; Downham, R.; Fazal, L.; Feltell, R.; Figueroa, E.; Frederickson, M.; Lewis, J.; McMenamin, R.; Murray, C. W.; O'Brien, M. A.; Parra, L.; Patel, S.; Phillips, T.; Rees, D. C.; Rich, S.; Smith, D. M.; Trewartha, G.; Vinkovic, M.; Williams, B.; Woolford, A. J. *J. Med. Chem.* **2010**, *53*, 5956.
13. Huang, K. H.; Veal, J. M.; Fadden, R. P.; Rice, J. W.; Eaves, J.; Strachan, J. P.; Barabasz, A. F.; Foley, B. E.; Barta, T. E.; Ma, W.; Silinski, M. A.; Hu, M.; Partridge, J. M.; Scott, A.; DuBois, L. G.; Freed, T.; Steed, P. M.; Ommen, A. J.; Smith, E. D.; Hughes, P. F.; Woodward, A. R.; Hanson, G. J.; McCall, W. S.; Markworth, C. J.; Hinkley, L.; Jenks, M.; Geng, L.; Lewis, M.; Otto, J.; Pronk, B.; Verleysen, K.; Hall, S. E. *J. Med. Chem.* **2009**, *52*, 4288.
14. Zhao, L.; Cao, D.; Chen, T.; Wang, Y.; Miao, Z.; Xu, Y.; Chen, W.; Wang, X.; Li, Y.; Du, Z.; Xiong, B.; Li, J.; Xu, C.; Zhang, N.; He, J.; Shen, J. *J. Med. Chem.* **2013**, *56*, 3833.
15. Halgren, T. A.; Murphy, R. B.; Friesner, R. A.; Beard, H. S.; Frye, L. L.; Pollard, W. T.; Banks, J. L. *J. Med. Chem.* **2004**, *47*, 1750.
16. Chodera, J. D.; Mobley, D. L. *Annu. Rev. Biophys.* **2013**, *42*, 121.
17. Marenich, A. V.; Cramer, C. J.; Truhlar, D. G. *J. Phys. Chem. B* **2009**, *113*, 4538.
18. Murray, C. W.; Carr, M. G.; Callaghan, O.; Chessari, G.; Congreve, M.; Cowan, S.; Coyle, J. E.; Downham, R.; Figueroa, E.; Frederickson, M.; Graham, B.; McMenamin, R.; O'Brien, M. A.; Patel, S.; Phillips, T. R.; Williams, G.; Woodhead, A. J.; Woolford, A. J. *J. Med. Chem.* **2010**, *53*, 5942.
19. Antilla, J. C.; Klapars, A.; Buchwald, S. L. *J. Am. Chem. Soc.* **2002**, *124*, 11684.
20. Hartwig, J. F.; Kawatsura, M.; Hauck, S. I.; Shaughnessy, K. H.; Alcazar-Roman, L. M. *J. Org. Chem.* **1999**, *64*, 5575.
21. Hanthorn, J. J.; Valgimigli, L.; Pratt, D. A. *J. Org. Chem.* **2012**, *77*, 6908.